

3D acoustic jet

Tuukka Kekkonen
Electronics lab., Physics dept.
University of Helsinki
Helsinki, Finland
tuukka.o.kekkonen@helsinki.fi

Joni Mäkinen
Electronics lab., Physics dept.
University of Helsinki
Helsinki, Finland
joni.mk.makinen@helsinki.fi

Jere Hyvönen
Electronics lab., Physics dept.
University of Helsinki
Helsinki, Finland
jere.hyvonen@helsinki.fi

Antti Kuronen
Accelerator lab., Physics dept.
University of Helsinki
Helsinki, Finland
antti.kuronen@helsinki.fi

Tapio Kotiaho
Dept. of Chemistry and Div.
Pharm. Chem. Technol.
University of Helsinki
Helsinki, Finland
tapio.kotiaho@helsinki.fi

Ari Salmi
Electronics lab., Physics dept.
University of Helsinki
Helsinki, Finland
ari.salmi@helsinki.fi

Edward Hæggström
Electronics lab., Physics dept.
University of Helsinki
Helsinki, Finland
edward.haeggstrom@helsinki.fi

Abstract—We demonstrate a way of focusing acoustic waves using a water immersed solid-solid lens. The focusing action is predicted by finite element simulations. This estimate is then compared to experiments. We use the lens to image a resolution sample and compare this image to one imaged with a comparable commercial immersion transducer.

Keywords—acoustic jet, ultrasonics, microscopy

I. INTRODUCTION

According to the Rayleigh criterion, the lateral resolution of an optical or acoustic system is limited by diffraction [1]. The theory predicts that it would be impossible to achieve a focal spot narrower than $\lambda/2$. Recent studies in optics show that this limitation can be circumvented by cleverly selecting the refractive index and the radius of a spherical lens, resulting in super resolution jets [2].

Circumventing the diffraction limit has been studied in the acoustic realm [3]. We showed previously that this phenomenon can be translated to the acoustics realm by using a cylinder immersed in a liquid to create a line focus narrower than $\lambda/2$ [4]. With a cylindrical lens, we conducted the experiment effectively in 2D. A similar study has been conducted by Pérez-López *et al.* where they used a water immersed sphere to create a 3D jet [5]. They were unable to achieve a focal spot narrower than $\lambda/2$ in their experiment.

In this study we present a water immersed ‘cup-lens’ geometry inspired by Hengyu *et al.* [6] to generate a 3D jet narrower than $\lambda/2$. We show a simulated intensity field and an experimental realization of the new lens structure.

II. METHODS

The acoustic lens consists of a solid 50 mm long steel cylinder with a hemispherical cavity coated with silver at one end (Fig. 1 & 2). The width of the focal spot was minimized by varying the radius of the cavity and the thickness of the coating in finite element method (FEM) simulations. The optimal radius was 6.59 mm and the thickness of the silver coating was 4.28

mm. The simulations were done in the frequency domain using COMSOL Multiphysics® (ver. 5.4) [7].

We conducted two different experiments. First, we mapped the acoustic field with a hydrophone (Fig. 1). Second, we imaged a resolution sample with a pulse-echo experiment (Fig. 2).

A. FEM-simulations

A 2D-axisymmetric simulation of the lens geometry was done in the frequency domain. COMSOL’s Solid Mechanics module was used to model the solid lens structure and the Pressure Acoustics module was used for the fluid domain. A transducer from the experiments was modeled as a boundary load (pressure) in the steel cylinder. The free edges of the solid domain were set to low reflecting boundaries to get rid of excess internal reflections. In the fluid domain, perfectly matched layers were used to effectively absorb the outward propagating waves from the domain. Meshing was done by setting the maximum mesh size to $\lambda/12$, tighter than the recommended value of $\lambda/6$. The mesh was further refined on the boundaries and in the region where the jet forms in the fluid.

B. Hydrophone experiment

To measure the acoustic field, a plastic container was glued to the focusing end of the acoustic lens and it was filled with degassed water. A contact transducer (Karl Deutsch S 12 HB 0,8-3) was placed under a translation stage (Isel: Isert-Electronic 6419) and the lens was placed on top of the transducer. A 3D printed holder made sure that the lens was properly pressed against the transducer. Finally, a hydrophone (Precision Acoustics SN2149, 1 MHz – 40 MHz) was suspended from the translation stage so that the tip of the hydrophone’s needle was close to the lens without touching it (Fig. 1).

A function generator (Analog Discovery 2, Digilent), connected to an amplifier (Mini-Circuits 15542) transmitted a 4-cycle sine burst with a frequency of 2.25 MHz and 25 V_{pp} amplitude. The signal was transmitted through the lens and picked up by the hydrophone. The signal was then amplified 40

dB (Panametrics 5660C), filtered by a custom 1.2 MHz high pass filter, and read by an oscilloscope (PicoScope 3403D).

A $(4 \times 4 \times 5) \text{ mm}^3$ -volume scan with $100 \mu\text{m}$ steps in x - and y -direction and $200 \mu\text{m}$ steps in z -direction was done to map the acoustic field. 100 4-cycle sine bursts were transmitted and averaged at each point.

C. Resolution sample pulse-echo experiment

For the resolution sample experiment, our set-up was mostly the same as described above. This time we suspended the contact transducer and the acoustic lens from the translation stage and placed a water-filled container below them. A heat sink with 1.3 mm wide fins and 7 mm wide gaps was placed in the container to act as a resolution sample (Fig. 2).

As for the electric circuit, a pulser (Panametrics 5058PR) excited the transducer with a negative delta spike. The signal was transmitted through the lens, reflected from the sample, and picked up by the same transducer. The received signal was amplified by the pulser and read by a 12-bit oscilloscope (LeCroy HDO4054A).

As before, the lens and the transducer were moved between each measurement point to scan a $(15 \times 5) \text{ mm}^2$ -plane 2.5 mm above the sample in $100 \mu\text{m}$ steps. The data was averaged over 100 signals.

Lastly, we imaged the same resolution sample with a focusing immersion transducer (Panametrics I3-0206-R, 2.25 MHz) to compare the image to the one obtained with our acoustic lens. The step length and the scan area were kept constant.

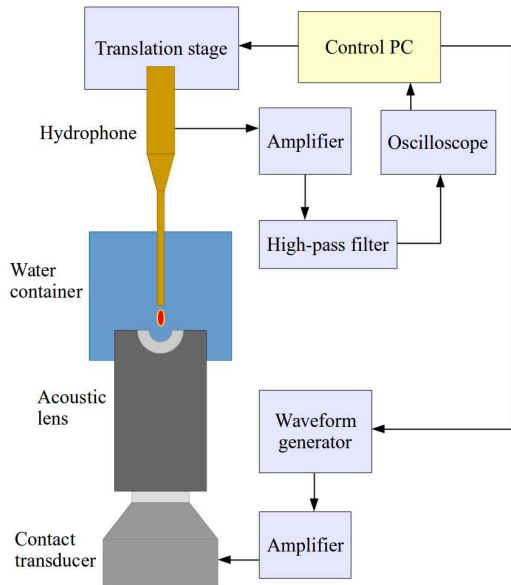


Fig. 1. Schematics of the set-up used in the hydrophone measurements. A 4-cycle sine burst was transmitted by the contact transducer. The acoustic lens consisting of a stainless steel cylinder and a silver hemisphere focuses the signal to a jet. A hydrophone scans a $(4 \times 4 \times 5) \text{ mm}^3$ -volume above the lens.

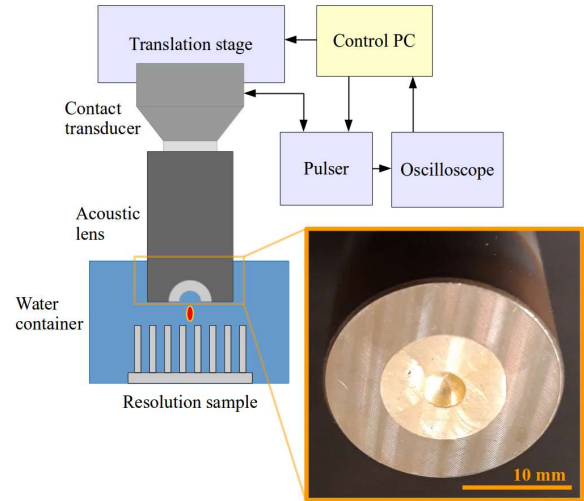


Fig. 2. Schematics of the the resolution sample experiment with a close-up photo of the lens. The contact transducer, excited by a delta spike, transmits a broadband acoustic signal through the acoustic lens. The signal is reflected from the resolution sample placed under the lens and picked up by the same contact transducer. The transducer and the lens are moved in steps to scan the sample.

III. DATA ANALYSIS

A. FEM-simulations

The width of the acoustic jet was determined at the intensity maximum. To do this, we fitted a gaussian function to the data, calculated the full width at half maximum (FWHM) of the gaussian (Fig. 3). The gaussian was fitted to 41 points closest the maximum amplitude value of the jet.

B. Hydrophone experiment

From the hydrophone signals, we extracted the first 4-cycle burst arriving to the hydrophone by analytically calculating the approximate time-of-flight. The data was time windowed with a window width three times the burst length. The windowed data was filtered using MATLAB's 'bandpass'-function ($2.25 \text{ MHz} \pm 0.3 \text{ MHz}$) and an envelope was computed from the filtered data. The focal signal was extracted from the maximum of the envelope. The width of the time window was kept long enough to contain the whole signal.

The extracted signal was squared and integrated over time. These values are presented in Fig. 4. The acoustic intensity was approximated as pressure squared.

C. Resolution sample pulse-echo experiment

The data from the acoustic lens experiment was analyzed as follows: Internal echoes were removed by measuring a reference signal without the presence of the sample and subtracting them from the pulse-echo data. To find the reflected signal from the data, we plotted a series of images (xy -planes) using a three-point moving average, and observed when the resolution sample became visible. For the immersion transducer experiment, the image was formed by integrating over the time signal of the focal echo.

To determine the resolution in both cases, the experimental data was compared to a convolution-based simulation. The theoretical shape of the convolution was obtained by convolving a gaussian, representing the acoustic beam profile, with a rectangular function, representing the resolution sample. The simulated convolution should match the measured profile.

IV. RESULTS

A. FEM-simulations

The acoustic pressure field simulated in FEM is presented in Fig. 3 and the FWHM at the intensity maximum was determined to be 0.47λ .

There is a difference between the shape of the simulated (Fig. 3) and measured (Fig. 4) fields. The difference between the simulated and the experimental acoustic field comes from the fact that the exact material properties are not known, and even a relatively small change in speed of sound affected the simulated results significantly. Also, the manufacturing defects in the lens alter the shape of the produced acoustic field, observed as asymmetries in Fig. 4.

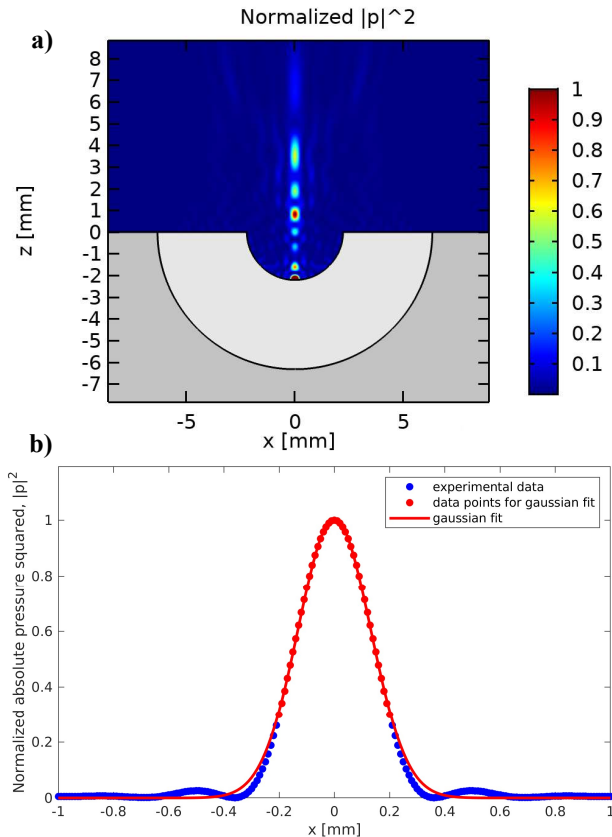


Fig. 3. a) FEM-simulated acoustic field (pressure squared) under the acoustic lens. The color axis is normalized to the maximum value. The simulation predicts that the jet is formed 0.7 mm above the lens. b) Gaussian function fitted to the maximum value of the simulated acoustic field. The gaussian is fitted only to the data points marked in red. The FWHM of the fit is 0.47λ .

B. Hydrophone experiment

The acoustic field is presented as a 3D plot to show that the jet really is three dimensional (Fig. 4). The FWHM was 0.45λ at the intensity maximum. This is below the $\lambda/2$ value.

The jet is 4-6 data points wide due to the long sampling interval along the x and y axes (Fig. 4). This makes plotting the gaussian to the data uncertain.

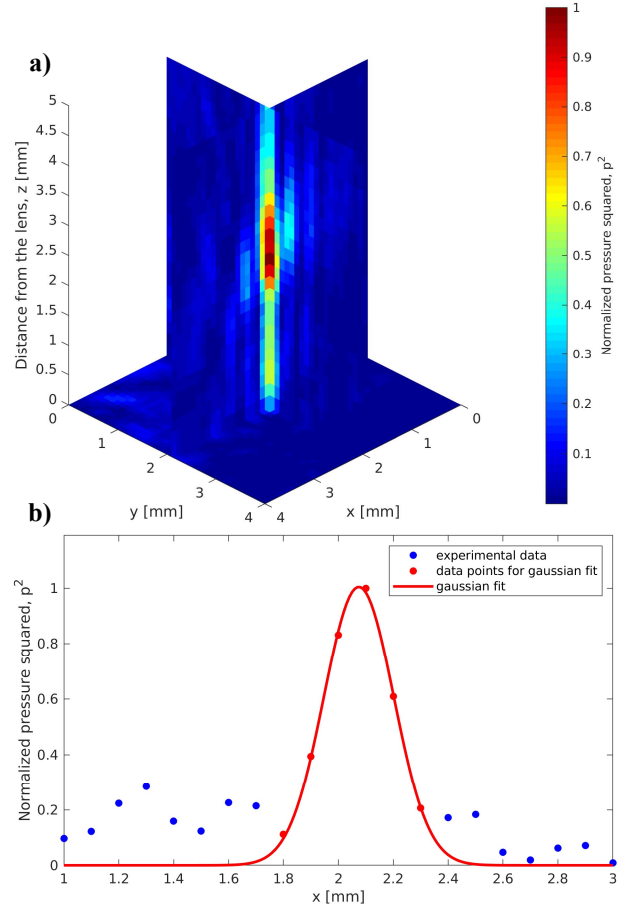


Fig. 4. a) Experimentally measured acoustic field (normalized pressure squared) above the lens. The maximum value of the jet is at 2.5 mm from the lens. In this plot, $z = 0.25 \pm 0.25$ mm is the point where the tip of the hydrophone needle is as close to the lens as we could get it without it touching the lens. b) Gaussian function fitted to the maximum value of the experimentally measured acoustic field. The FWHM of the gaussian is 0.45λ .

C. Resolution sample experiment

The images generated by the acoustic lens and the commercial immersion transducer are presented in Fig. 5. In Fig. 6 we compare the simulated convolution with the B-line from the middle of the C-scan (Fig. 5). For the immersion transducer, the theoretical FWHM of the acoustic beam calculated from the numerical aperture is 2.0 mm. We estimated the resolution of the of the immersion transducer by varying the FWHM of the simulated gaussian so that the simulated convolution would match the experimental B-line. The best match was achieved with a FWHM of 2.5 mm suggesting that the sample was off-focus.

For the lens structure, the simulated convolution correctly predicts that the peak of the B-line is flat. However, since we used a gaussian function for the convolution, the simulation does not account for the contribution of the side lobes. There is asymmetry both in the B-line (Fig. 6) and in the measured acoustic field (Fig. 4). Since the B-line measured with our lens structure matches the simulated convolution with the flat peak, we conclude that the resolution of the lens structure is higher than the resolution of the immersion transducer. We justify this comparison by showing that their frequency contents are comparable (Fig. 7).

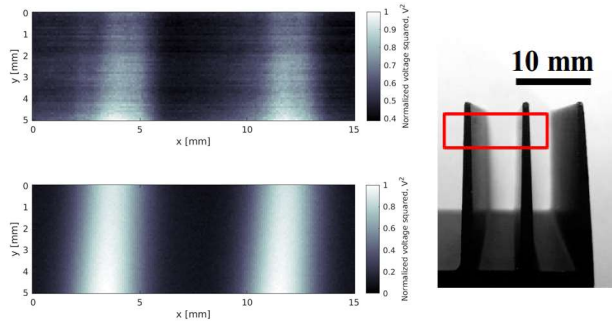


Fig. 5. Amplitude C-scans used to determine the resolution of our lens structure (top) and the immersion transducer (bottom). On the right: photograph of the resolution sample, the red rectangle represents the imaged area.

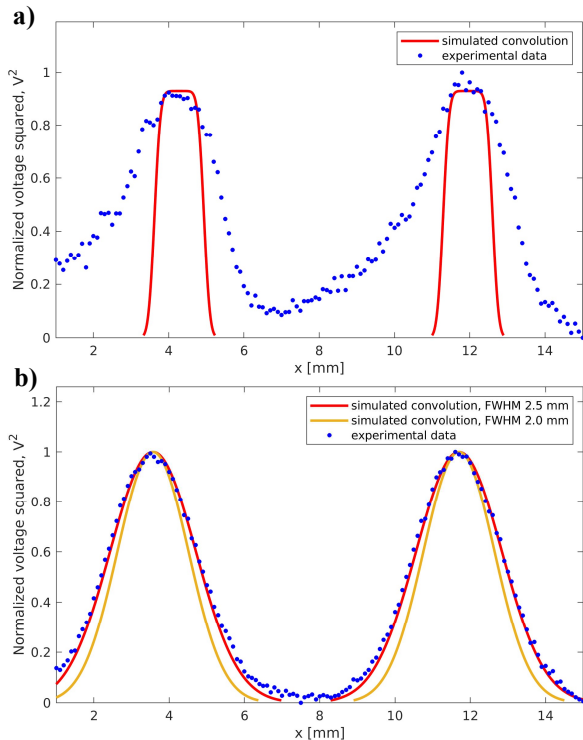


Fig. 6. Comparison between the simulated convolution of a gaussian (acoustic beam) with a rectangular function (resolution sample) and the measured B-line for a) our lens b) the immersion transducer. Convolution was calculated by multiplying the width of the resolution sample by a gaussian of assumed FWHM: 0.3 mm ($= 0.45\lambda$) with our lens and 2.5 mm with the immersion transducer.

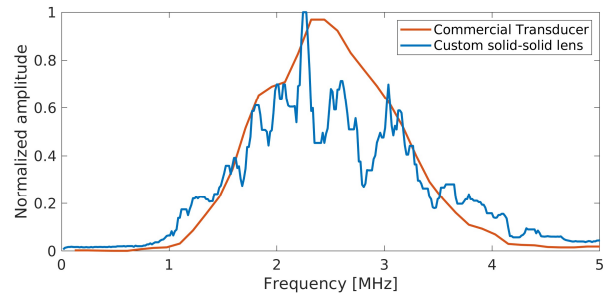


Fig. 7. Frequency contents for the focusing transducer and our lens structure. These spectra justify the comparison between the two experiments to determine the wavelength-limited resolution in Fig 6.

V. CONCLUSIONS

We demonstrated a technique to translate the optical, sub $\lambda/2$ 3D jet to the acoustic realm using a solid-solid lens structure immersed in water. We showed that this structure can be used as an extension to a commercial contact transducer to image a water immersed sample.

REFERENCES

- [1] L. R. Rayleigh, "Investigations in optics, with special reference to the spectroscope," *Mag. J. Sci.*, vol. 8, pp. 261–274, 1879.
- [2] Z. Chen, A. Taflove and V. Backman, "Photonic nanojet enhancement of back scattering of light by nanoparticles: a potential novel visible-light ultramicroscopy technique," *Opt. Express*, vol. 12, 1214, 2004.
- [3] O. V. Minin, I. V. Minin, "Acoustojet: acoustic analogue of photonic jet phenomenon based on penetrable 3D particle," *Opt. Quantum Electron.*, vol. 49, 54, 2017.
- [4] D. Veira Canle *et al.*, "Practical realization of a sub- $\lambda/2$ acoustic jet," *Sci. Rep.*, vol. 9, 5189, 2019.
- [5] S. Péres-López *et al.*, "Liquid-liquid core-shell configurable mesoscale spherical acoustic lens with subwavelength focusing," *Appl. Phys. Express*, vol. 12, 8, 2019.
- [6] Z. Hengyu, C. Zaicun, C. T. Chong, H. Minghui, "Photonic jet with ultralong working distance by hemispheric shell," *Opt. Express*, vol. 5, pp. 6626–6633, 2015.
- [7] COMSOL Multiphysics® v. 5.4. www.comsol.com. COMSOL AB, Stockholm, Sweden.